Transactions on Electrical and Electronic Materials (2024) 25:371–379
https://doi.org/10.1007/s42341-024-00536-1

Online ISSN 2092-7592
Print ISSN 1229-7607

REVIEW PAPER

Approaches to Improve Mobility and Stability of IGZO TFTs: A Brief Review

Zhong Pan[1] · Yifan Hu[1] · Jingwen Chen[1] · Fucheng Wang[1] · Yeojin Jeong[1] · Duy Phong Pham[1] · Junsin Yi[2]

Received: 30 October 2023 / Revised: 17 March 2024 / Accepted: 30 March 2024 / Published online: 26 April 2024

Abstract

Among metal oxide material TFTs, IGZO TFTs are highly regarded for their exceptionally high mobility, exceeding 10 $cm^2/V{\cdot}s$, remarkable transparency of more than 80%, and their adaptable low-temperature fabrication techniques. High-performance displays operating at refresh rates of up to 144 Hz and undergoing millions of device switches demand IGZO TFTs with mobility exceeding 20 $cm^2/V{\cdot}s$ and higher stability against impulse stress. The effect of IGZO material composition on device stability and recent strategies to promote the mobility and stability of IGZO TFT by modifying the transistor structure, preparation process, and post-processing techniques to reduce V_O have been discussed. The paper describes the application of IGZO TFTs in flexible electronics.

Graphical Abstract

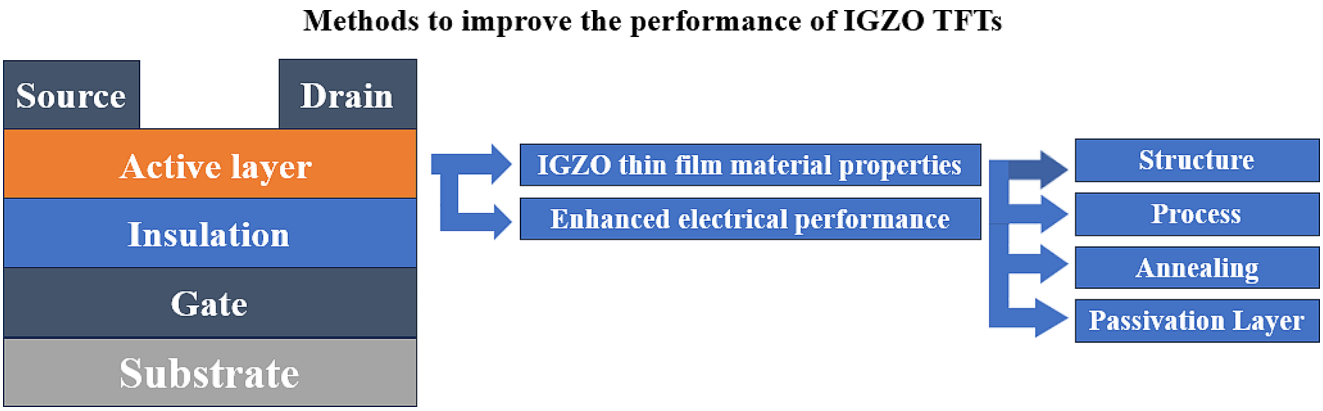

Keywords Thin film transistor · Oxygen vacancy · IGZO · Process · Annealing · Passivation layer

1 Introduction

Thin film transistors (TFTs) serve as a critical component employed for pixel control in active-matrix liquid crystal displays (LCDs) [1]. Conventional liquid crystal displays typically utilize silicon-based TFTs, including amorphous silicon (a-Si) TFTs and polycrystalline silicon (p-Si) TFTs [2].

With the advancement of high-definition display technology, there has been a surge in interest in oxide semiconductors, particularly in the domain of amorphous oxide semiconductors. As illustrated in Table 1, thin-film

✉ Duy Phong Pham
pdphong@skku.edu

✉ Junsin Yi
junsin@skku.edu

[1] Department of Electrical and Computer Engineering, Sungkyunkwan University, Suwon 16419, Republic of Korea

[2] College of Information and Communication Engineering, Sungkyunkwan University, Suwon 16419, Republic of Korea

Table 1 Comparison of electrical properties and preparation temperatures of polysilicon and amorphous silicon and IGZO TFTs [15–18]

	a-Si: H	Poly-Si	Metal oxide semiconductor
Channel	a-Si: H	ELA/SPC	a-IGZO
Mobility ($cm^2/V·s$)	0.1 ~ 1	30 ~ 100	10 ~ 100
V_{th} shift	> 10 V	< 0.5 V	< 1.5 V
Light stability	Weak	Good	Medium
Preparation temperature	150–350 °C	250–550 °C	25 ~ 350 °C

transistors (TFTs) fabricated from oxide semiconductors demonstrate significantly higher carrier mobility and superior uniformity compared to traditional silicon-based counterparts. Metal oxide semiconductor TFTs typically exhibit excellent bias stability, with the failure mechanism primarily associated with interfacial states and oxygen defects. IGZO boasts a high electron mobility ranging from 10 to 30 cm^2/Vs and remarkable visible light transmittance, surpassing that of most other oxide semiconductors.

Furthermore, they can be fabricated under ambient room temperature conditions [3]. In 2004, Nomura et al. [4] demonstrated a-IGZO Amorphous Indium Gallium Zinc Oxide (a-IGZO) TFT. The field-effect mobility(μ_{FE}) of a-IGZO TFTs can reach 160 $cm^2/V·s$, which is a significant improvement over that of a-Si TFTs [5]. Therefore, it is considered the mainstream material for the next generation flat panel display technology [6–13]. While IGZO TFTs boast exceptional electrical properties, their stability has become a critical concern, impeding their widespread commercial adoption. The stability of IGZO TFTs is notably influenced by both the oxygen content within the IGZO material and environmental conditions [14]. As the IGZO active layer is prone to defective states and impurities, the device is susceptible to adverse phenomena such as threshold voltage drift, and increased sub-threshold swing under electric field and light conditions, thus affecting the reliability of the device and circuit. This requires not only controlling the intrinsic defects of the materials themselves, but also optimizing the structural design and process flow of the devices to suppress failure mechanisms such as carrier capture and interface state formation.

In summary, improving the mobility and stability of IGZO TFTs to achieve high performance and high reliability is the current difficulty in the commercialization of IGZO. This review aims to comprehensively summarize the research progress on improving the mobility and stability of IGZO TFTs in recent years, including various strategies such as structural optimization, improvement of process conditions, and to look forward to the future direction of development.

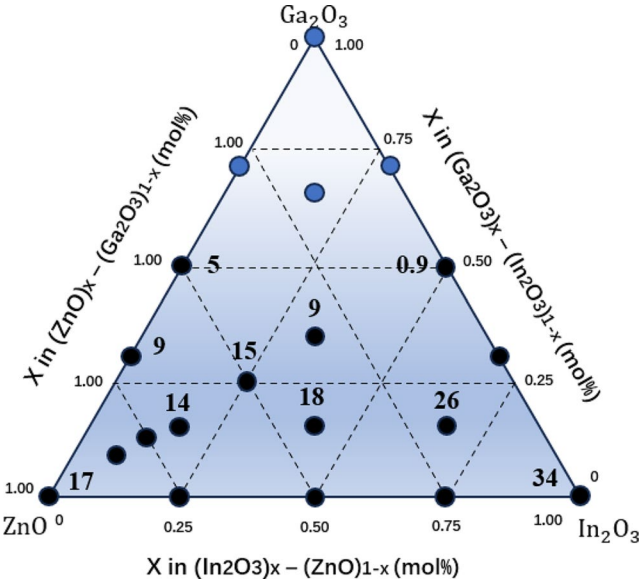

Fig. 1 Carrier transport properties of IGZO films with different ratios, values indicate electron Hall mobility ($cm^2V^{-1}s^{-1}$) [20]

2 Oxygen Vacancy in the IGZO Active Layer

Oxygen vacancies (V_O) are among the most common defects found in semiconductors, especially in metal oxide semiconductors, and they play a significant role in shaping the performance of semiconductor devices [19]. IGZO materials consist of oxides comprising three primary elements: Indium (In), Gallium (Ga), and Zinc (Zn). Altering the ratio of these three elements can lead to variations in the properties of the IGZO material.

As shown in Fig. 1 [20], The presence of indium ions enhances carrier mobility and conductivity owing to the large orbital radius of indium and the significant overlap of ns orbitals between neighboring atoms. But the low bond energy of the In-O bond makes the In-O bond less stable, and it is possible for oxygen atoms to move from their crystalline positions, leaving an oxygen vacancy. These vacancies can become trapping centers for electrons and holes, thus reducing the mobility of the material. But this part of the effect is small, and the overall mobility of the IGZO film is up as the In2O3 content increases [21]. The low carrier concentration of IGZO is attributed to the high ionic potential of Ga^{3+}, which allows Ga^{3+} to bind tightly with O^{2-} and helps inhibit the generation of V_O, thus reducing the concentration of free electrons [22]. The Zn^{2+} has a stable tetrahedral structure to maintain the amorphous structure of IGZO.

Table 2 Development status and performance of dual active layer TFT

Material	Pre-Mobility	Mobility($cm^2/V\cdot$)	V_{th}drift(V)	Subthreshold Swing(mV/decad)	References
ZnO: H/ZnO	6.52	12.1	-4	670	[23]
IGTO/IZO	0.27	4.38		550	[24]
IGZO/IZO		40	-0.07		[25]
IGZO/Ga2O3	11.5	22.2			[26]
IAZO/IAZO	12.05	19.56	1.24		[27]
a-IZO/IGZO	10.3	50	2.3	180	[28]
IGZO/IGZO	10.1	23.4		170	[29]
IGZO/ZTO	11.7	20.4		110	[30]
IGZO/IGZO		5.41		95	[31]

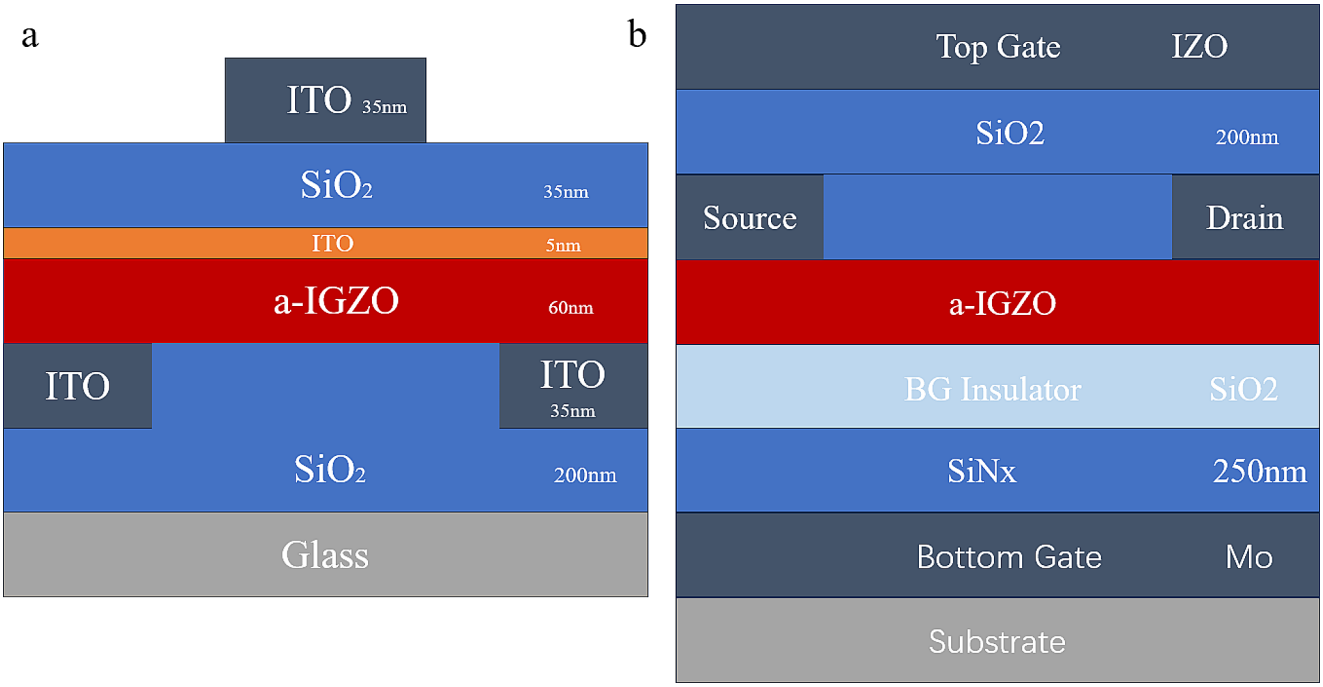

Fig. 2 (**a**) ITO/IGZO TFTs device structure and (**b**) IZO/Mo Dual-Gate structure [33, 34]

3 Recent Advances in IGZO Thin Film Transistor

Many factors influence the mobility and stability of IGZO TFTs. This paper concentrates on the structure and preparation process of TFTs to investigate the alterations in TFT properties.

3.1 Improved Properties Through Structure

Dual-Active Layer is a type of TFT structure used to improve the electrical properties of TFTs. The principle is to introduce two varied materials or layers into the TFT structure, one of which is used to provide high mobility, and the other is used to provide a stable carrier concentration. Table 2 demonstrates the relevant papers and electrical properties of dual-active layer thin film transistors.

The Dual-Active Layer TFT structures involving both Indium Zinc Oxide (IZO) and IGZO were initially reported by Kim et al. in 2008 [32]. The electron mobility reached 104 cm ^{2}V $^{-1}$s $^{-1}$ and excellent stability was achieved under gate stress. In 2021, Mohammad Masum Billah et al. [28] demonstrated a Dual-Active Layer TFT(a-IGZO/a-IZO) with a coplanar structure. They found that compared with a single layer a-IGZO TFT whose μ_{FE} is about 10 $cm^2/V\cdot s$, the Dual-Active Layer structure improves flowability up to about 50 $cm^2/V\cdot s$.

The Dual-Active Layer structure can also greatly improve the stability of TFT. In 2022, Cong Peng and their team deposited an oxygen-rich ITO layer onto the IGZO layer using PECVD to create a top gate Dual-Active Layer TFT [33]. The structure is shown in Fig. 2(a).

The findings indicate that the high carrier concentration oxygen-rich ITO film has a substantial impact on the performance of the ITO/IGZO TFT. The negative bias illumination

stress (NBIS) test results are shown in Fig. 3. The threshold voltage exhibits a drift with prolonged illumination and gate bias time. According to the experimental results, the ITO/IGZO TFT exhibits a lower threshold voltage drift (ΔV_{th}) in comparison to the IGZO TFT when subjected to illumination and gate bias stress. This phenomenon could be attributed to the ionization of oxygen vacancies (V_O) defects in IGZO films induced by the sputtering of ITO films [35]. Under NBIS Vo loses two electrons and is converted to V_O^{2+}. V_O^{2+} gains electrons back to V_O still overcoming the 0.2–0.3 eV barrier, then Vth will return to its original position after some time after NBIS is withdrawn. However, in fact, it is difficult to return to the original position even after NBIS is withdrawn for several days, which suggests that V_O^{2+} is in a sub-stable state. The oxygen vacancy migration model suggests that the oxygen vacancy defects can move, and the recovery of NBIS needs to cross the intermediate-phase barrier of Oi (which is as high as 0.65–0.75 eV for IGZO), so it takes a long time to recover [22, 36].

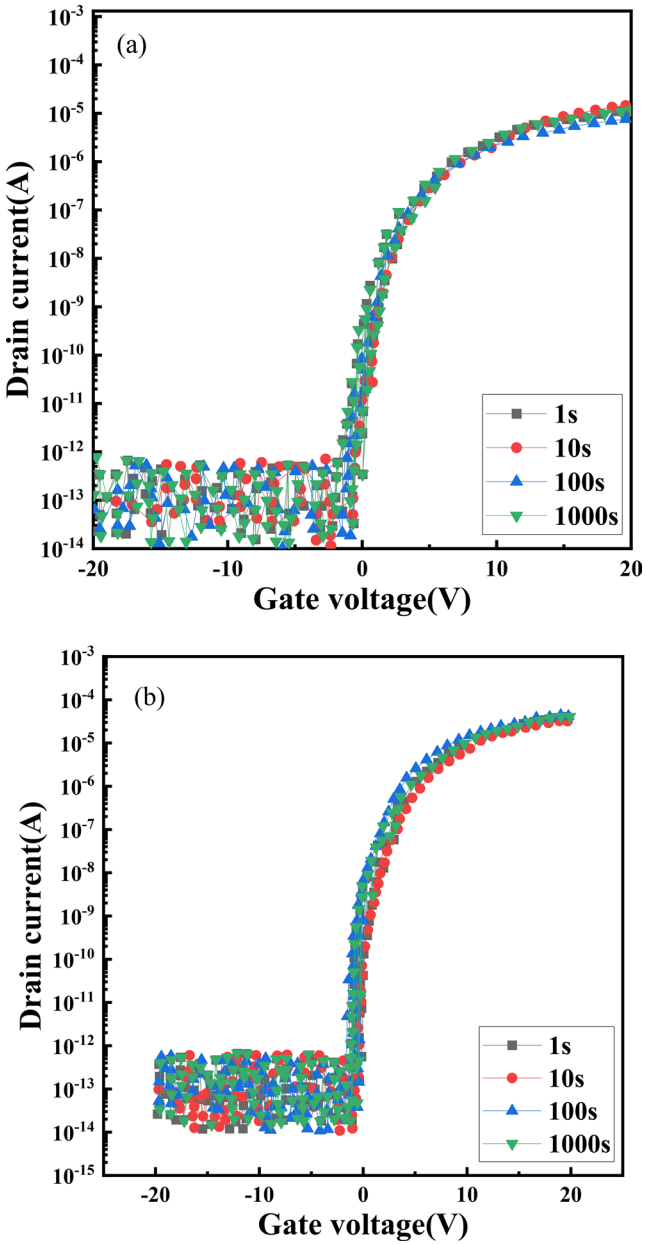

Fig. 3 Transfer characteristic curves of IGZO TFT under NBIS: (**a**) IGZO TFT (**b**) ITO/IGZO TFT [33]

In addition to modifying the channel, changing the characteristics of the TFTs by adding a gate is also an effective method. Mohammad Masum Billah et al. [34] devised an a-IGZO TFT featuring a Dual-Gate configuration and conducted a comparative analysis of stability between Single-Gate and Dual-Gate structures. The structure is shown in Fig. 2(b). Their findings revealed that the displacement of ΔV_{th} in Dual-Gate TFTs under NBIS was significantly reduced in comparison to single-gate TFTs. The enhanced stability of the Dual-Gate-driven TFT can be elucidated by the rapid shifting of the quasi-Fermi energy levels in a-IGZO induced by the Dual-Gate drive. This effect becomes more pronounced, particularly as the thickness of the active layer decreases [37].

Additionally, their research confirmed that a-IGZO TFTs with thinner active layers exhibited higher stability under NBIS compared to those with thicker active layers. Sunaina Priyadarshi et al. [38] assessed the impact of impulse stress on the stability of Single-Gate and Dual-Gate TFTs. They applied a positive gate pulse voltage ranging from 0 to 30 V, with a ΔV_{th} of 1.3 V for Dual-Gate TFTs and 2.4 V for Single-Gate TFTs. As the frequency increased, they observed that Dual-Gate TFTs exhibited a ΔV_{th} drift of 1.8 V, whereas Single-Gate TFTs displayed a ΔV_{th} of 3.0 V. These results suggest that Dual-Gate TFTs demonstrate greater stability when subjected to positive gate pulse voltage stress. The primary cause of device degradation is believed to be electron trapping at the interface between the active channel and gate insulator, along with the formation of defects within the bandgap.

3.2 Improvement of TFT Properties by Active Layer Fabrication Process

The use of different preparation processes for the active layer of IGZO TFTs may also have an impact on the performances of the TFTs.

In 2020 Jaemin Kim et al. [39] prepared IGZO films of 30 nm thickness that were produced at room temperature using radio-frequency magnetron sputtering (RF) and pulsed direct current magnetron sputtering (Pulsed-DC) techniques and annealed for 1 h in an air environment. Their mobilities were 18.20 $cm^2/V{\cdot}s$ and 13.06 $cm^2/V{\cdot}s$, respectively. The positive bias stress (PBS) and negative bias stress (NBS) test results are shown in Fig. 4.

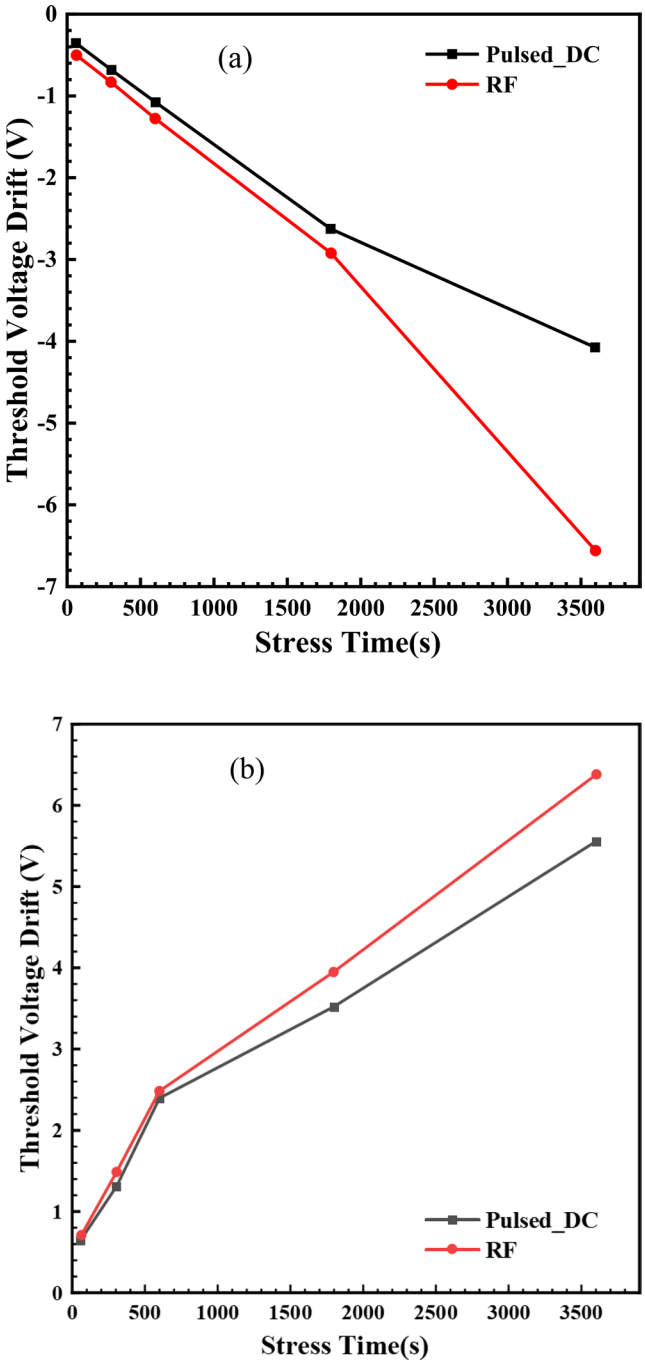

Fig. 4 Bias stress test result of pulsed-DC(black) and RF(red) under(**a**) NBS (**b**)PBS [39]

From the results, the ΔV_{th} shift of the TFTs prepared with pulsed-DC is smaller than that of the TFTs prepared with RF under both positive and negative bias conditions. A similar study was conducted by Wei-Sheng Liu et al. [40]. They similarly observed that the mobility and stability of IGZO TFTs prepared by pulsed DC magnetron sputtering were superior to that of RF magnetron sputtering. This enhancement can be ascribed to the capacity of pulsed DC magnetron sputtering to regulate plasma density by reducing sputtering power and adjusting pulse frequency, thus constraining arc discharges. Consequently, this approach yields a more uniform film with reduced impurity content.

In 2019, Min Hoe Cho et al. investigated the mobility and stability of IGZO TFTs by RF and Atomic Layer Deposition(ALD) [41]. The positive bias drift of the TFT prepared by sputtering is 1.7 V and the negative bias drift is -0.5 V. In contrast, the ΔVth values shifted by 0.5 V and − 0.5 V after applying PBS and NBS to the TFT prepared by the ALD process, respectively. Simultaneously, the mobility of TFTs employing ALD is 16.5 cm²/V·s higher than that of devices fabricated using sputtering. This difference is likely because the ALD process results in fewer trap-like V_O defects compared to the sputtering process. The ALD technique allows for single-layer atomic and molecular precision and can provide excellent uniformity. However, high cost and low deposition rates limit its large-scale application [42].

The mobility and stability are also influenced by the target material and sputtering conditions in magnetron sputtering. Jun Young Huh et al. found that IGZO TFTs with higher Ga content show more stable performance under bias stress however higher Ga content decreases the mobility of IGZO TFTs [43]. The bonding between Ga ions and oxygen ions is stronger than that between Zn and oxygen ions. Therefore, as the Ga content increases, the number of oxygen vacancies in IGZO tends to decrease, thereby enhancing stability. Dae Gyu Yang adjusted the flow rate of Ar: O_2 during sputtering and found that the mobility and stability of the TFTs deteriorated with the increase in the flow rate of Ar gas [44]. These process findings will contribute to enhancing the performance and expanding the application range of IGZO TFTs.

3.3 Improved Performance Through Annealing

Annealing treatment is widely acknowledged as a crucial method for enhancing device performance, as the defect states in metal oxide materials can be influenced by both the annealing temperature and the surrounding atmosphere.

In 2021, Tiantian Pi et al. [45] reported a strategy to enhance the mobility of a-IGZO TFT using microwave annealing (MWA). MWA technology is a method of processing semiconductor devices using microwave radiation, which generates heat by exciting molecular vibrations in the material. The μ_{FE} of TFTs can be increased to 29.2 cm²/V·s using microwave annealing. In addition, MWA annealing of the TFTs effectively improves the stability, and after 5 min of treatment at 840 W MWA annealing, the TFTs have the smallest ΔV_{th} value and show excellent stability under NBS or PBS conditions. The advantage of MWA is that it allows

for rapid warming of the device and uniform heating of the device, reducing temperature gradients and thermal stresses in the material. The MWA treatment reduces the density of trap states associated with V_O by inducing a rearrangement of V_O which facilitates an increase in the electron mobility of the material.

In addition to enhanced annealing techniques, employing a multi-step annealing process is also a viable option. Cong Peng et al. [46] successively annealed the active layer and the finished device of IGZO TFT. Figure 5 shows the test results. From the results, the highest mobility (16.75 cm²/V·s) and lowest threshold voltage (1.27 V) were observed at room temperature with pre-annealing and 300 °C post-annealing. Threshold voltage shift was found to be minimized at 200 °C for pre-annealing and 300 °C for post-annealing. The device's PBS deteriorates when the temperature exceeds 400 °C. NIBS testing of the devices revealed the hump was significantly smaller for the TFTs with a post-annealing temperature of 300 °C than for the device with a post-annealing temperature of 200 °C. The enhancement in the stability of IGZO TFTs with two-step annealing may be attributed to the infusion of H, which fills the oxygen vacancies (V_O) within the IGZO layer and effectively passivates the defects between the insulating layer and the active layer [47]. From the experimental results, it is easy to see that two-step annealing is an amazingly effective strategy for enhancing the stability of IGZO TFTs.

Tianyuan Song et al. [48] employed oxygen annealing to alleviate localized degradation in IGZO TFTs subjected to AC gate bias stress. When the stress time is 3000 s and the stress amplitude is 20 V, the displacements of the transfer curve are 6.3 V and 14.2 V, respectively. Experimental results show that annealing at 400 °C in an oxygen environment reduces metal-hydrogen formation and metal-metal bonds in V_O.

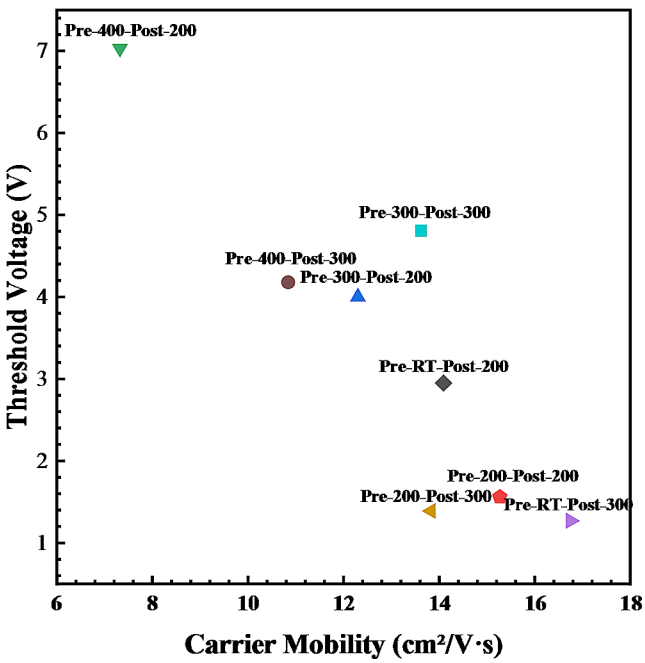

Fig. 5 Threshold voltage and mobility of IGZO TFT at different annealing temperatures [46]

Yiran Wei et al. [49] observed that a-IGZO TFTs, when annealed at 300 °C in a nitrogen atmosphere for one hour, exhibited source-drain short circuits attributed to the generation of a significant number of V_O. However, when the temperature in the N_2 atmosphere was reduced to 200 °C, a decrease in V_O within the IGZO active layer was observed. Furthermore, devices annealed at 200 °C in a nitrogen atmosphere, when subsequently annealed at 300 °C, were found to be free of short circuits. This could be attributed to the substitution of oxygen ions, involved in weak metal-oxygen bonds, by nitrogen atoms during the 200 °C nitrogen annealing process.

Based on the above analysis, it is apparent that employing multiple annealing processes and altering the gas atmosphere during annealing can effectively inhibit the formation of V_O in the active layer of IGZO.

3.4 Improvement of TFT Performance Using Passivation Layer

Given the susceptibility of metal oxide materials to airborne environments containing elements such as O_2, H_2, and H_2O, it is essential to fabricate a high-quality thin film as a passivation layer for TFTs.

CYTOP (Cyclic Olefin Polymer) is a high-performance polymer with excellent chemical stability and low surface energy. Kyung-Mo Jung et al. [50] in 2020 reported a way to promote the stability of a-IGZO TFTs using CYTOP material as a passivation layer. The structure is shown in Fig. 6. Their study found that during the annealing process, the fluorine in CYTOP diffuses into the IGZO film and effectively passivates the V_O defects therein. As a result, this passivation layer serves to prevent the deterioration of the electrical properties of the TFT device when subjected to PBS, NBS, and NBIS conditions. In 2021, Yuanbo Li et al. [51] used AlO_x material as a passivation layer for IGZO TFTs. The interfacial layer will be formed between AlO_x and the IGZO channel, and at the same time, Al ions during the deposition process will break the indium-oxygen bond in the IGZO film, When the bond between indium and oxygen is disrupted, defects, primarily oxygen vacancies, emerge within the IGZO lattice. These vacancies can serve as shallow donor impurities, introducing additional carriers (electrons) into the material, which can enhance the mobility of the TFT device.

Most researchers in the past used inorganic materials as passivation layers such as SiO_2, Al_2O_3, and so on. In

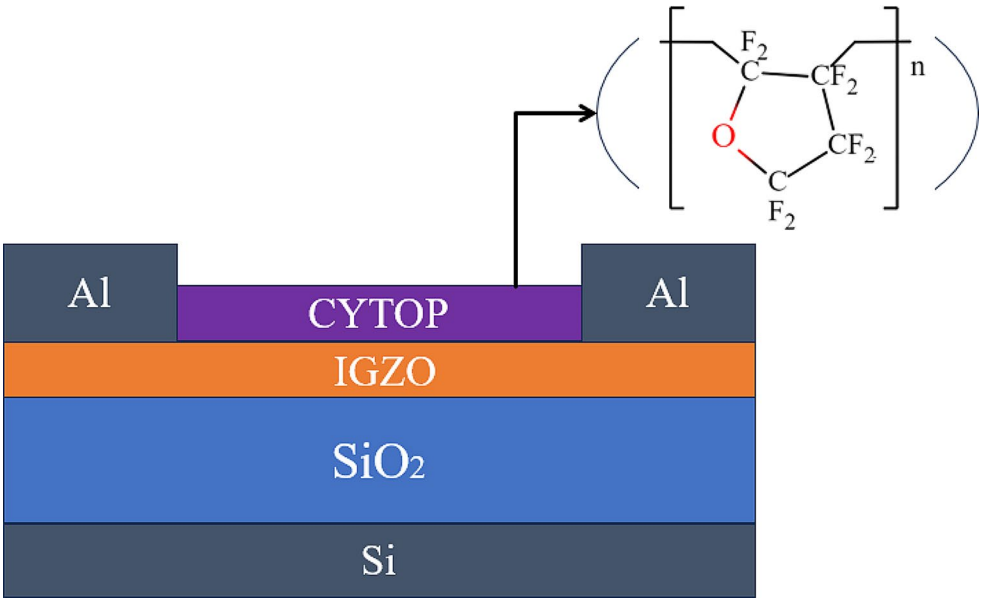

Fig. 6 IGZO TFT structure with CYTOP passivation layer [34]

recent years, the use of organic materials has been increasingly reported. Kwan Yup Shin et al. [52] proposed the use of Nitrocellulose (NC) as a passivation layer using spin coating. The use of an NC passivation layer increases the mobility to more than 20 $cm^2/V{\cdot}s$ and reduces the threshold voltage to 0.56 V. The ΔV_{th} under the PBS test was reduced by 2.73 V. These improvements are attributed to the diffusion of nitrogen from the NC passivation layer into the a-IGZO channels. There are weakly bonded oxygen atoms inside the a-IGZO channel layer, and this weakly bonded oxygen can easily cause lattice defects and energy level traps. The nitrogen atoms diffused into the layer have stronger electronegativity than the oxygen atoms and can preferentially form more stable bonds with the surrounding metal cations, thus reducing the oxygen vacancies.

4 Application Prospects of IGZO TFT

Since 2010, the application of IGZO TFTs in LCD and OLED panels has been gradually increasing [53], and IGZO TFT has the advantages of high electron mobility and fast response speed, which are in line with the requirements of high-resolution liquid crystal displays. Hong-Jae Shin et al. [54] proposed an 8 K OLED display technology using IGZO TFT, which successfully improved the image quality of 8 K OLED displays. Yujiro Takeda et al. [55] prepared a top-gate structure IGZO TFT and applied it to a 12.3-inch ultra-wide flexible display. The device can maintain good working conditions in 85 °C high temperature, -30 °C low temperature, and 60 °C temperature and humidity 90% environment.

The superior mechanical bending properties of IGZO TFTs can be utilized to create curved displays such as e-paper [20, 53, 56], and folding screens [57, 58]. Baixiang Han et al. [59] presented a 17-inch foldable printed OLED display based on a flexible IGZO-TFT backplane. The OLED display achieves a brightness of 400 nits, a uniformity of more than 90%, and a bending radius of 4 mm.

The sensitivity of IGZO TFTs to light, pressure, and some gases allows them to be used in the field of sensors. Mani Teja Vijjapu et al. [60] in 2021 reported the detection of NO_2 by utilizing a solution-treated IGZO TFT gas sensor at room temperature. Wenya Jiang et al. [61] prepared IGZO TFTs with chitosan (CS) gate dielectrics using photolithography. These CS-based transparent IGZO TFTs are sensitive to glucose and can be used to detect glucose concentration, which can be widely used in biomedical applications.

5 Conclusion

This paper provides a concise overview of several methods for enhancing the mobility and stability of IGZO transistors. The findings indicate that both dual active layers and dual gate structures effectively enhance the mobility and stability of TFT devices. A comparison of various preparation processes reveals that IGZO TFTs prepared by pulsed DC magnetron sputtering exhibit smaller threshold voltage drift and superior stability in comparison to IGZO TFTs prepared by RF magnetron sputtering, particularly under positive and negative bias stress conditions. Furthermore, adjusting the ratio of IGZO target to oxygen content can improve TFT stability, and ALD-prepared TFTs demonstrate fewer oxygen vacancy defects compared to those prepared via magnetron

sputtering. Annealing processes are effective in mitigating defects between the channel and the gate. The application of either organic or inorganic protective layers contributes to enhanced TFT stability. Lastly, the paper presents the diverse applications of IGZO TFTs in various fields.

Funding This work was supported by the National Research Foundation of Korea (NRF) grant funded by the Korea government (MSIT) (No. NRF-2022R1A4A1028702). This work was also supported by the Technology Innovation Program (or Industrial Strategic Technology Development Program) (RS-2023-00266568) funded by the Ministry of Trade, Industry & Energy (MOTIE, Korea).

Declarations

Conflict of interest There is no existing conflict of interests.

References

1. A. Nathan, K. Sakariya, A. Kumar, P. Servati, K.S. Karim, D. Striakhilev, A. Sazonov, in *Proceedings of the IEEE 2003 Custom Integrated Circuits Conference*, 2003. (IEEE, 2003), pp. 215
2. R. Chen, W. Zhou, M. Zhang, M. Wong, H.S. Kwok, IEEE Electron Device Lett. **34**, 60 (2012). [doi]
3. J.-Y. Kwon, D.-J. Lee, K.-B. Kim, Electron. Mater. Lett. **7**, 1 (2011). [doi]
4. K. Nomura, H. Ohta, A. Takagi, T. Kamiya, M. Hirano, H. Hosono, *nature* 432, 488 (2004). [doi]
5. H.-W. Zan, C.-C. Yeh, H.-F. Meng, C.-C. Tsai, L.-H. Chen, Adv. Mater. **24**, 3509 (2012). [doi]
6. S.Y. Lee, Trans. Electr. Electron. Mater. **21**, 235 (2020). [doi: 10.1007/s42341-020-00197-w]
7. J.S. Park, W.-J. Maeng, H.-S. Kim, J.-S. Park, Thin Solid Films. **520**, 1679 (2012). https://doi.org/10.1016/j.tsf.2011.07.018]
8. J. Raja, K. Jang, C.P.T. Nguyen, J. Yi, N. Balaji, S.Q. Hussain, S. Chatterjee, Trans. Electr. Electron. Mater. **16**, 234 (2015). [doi]
9. K. Walsh, N.E. Gorji, Results Phys. **56**, 107233 (2024). [doi]
10. X. Yu, Y. Shang, L. Zheng, K. Wang, ACS Appl. Electron. Mater. **5**, 5240 (2023). [doi]
11. Y. Liu, L. Wang, D. Li, K. Wang, Prot. Control Mod. Power Syst. **8**, 1 (2023). [doi]
12. X. Yu, N. Ma, L. Zheng, L. Wang, K. Wang, *Technologies* 11, 42 (2023). [doi]
13. J. Gao, D. Yang, S. Wang, Z. Li, L. Wang, K. Wang, J. Energy Storage. **73**, 109248 (2023). [doi]
14. W.-T. Chen, S.-Y. Lo, S.-C. Kao, H.-W. Zan, C.-C. Tsai, J.-H. Lin, C.-H. Fang, C.-C. Lee, IEEE Electron Device Lett. **32**, 1552 (2011). [doi]
15. T. Kamiya, K. Nomura, H. Hosono, Sci. Technol. Adv. Mater. (2010). [doi]
16. E. Fortunato, P. Barquinha, R. Martins, Adv. Mater. **24**, 2945 (2012). [doi]
17. Y.S. Rim, H. Chen, B. Zhu, S.H. Bae, S. Zhu, P.J. Li, I.C. Wang, Y. Yang, Adv. Mater. Interfaces. **4**, 1700020 (2017). [doi]
18. K. Myny, Nat. Electron. **1**, 30 (2018). [doi]
19. H. Meng, S. Huang, Y. Jiang, Inform. Technol. **1**, 2 (2020). [doi]
20. T. Kamiya, H. Hosono, NPG Asia Mater. **2**, 15 (2010). [doi]
21. Y.-H. Lin, J.-C. Chou, J. Nanomaterials. **16**, 442 (2015). [doi]
22. L. Lin-Feng, Z. Peng, P. Jun-Biao, Acta Phys. Sinica **65** (2016). [doi]
23. D. Wang, Z. Jiang, L. Li, D. Zhu, C. Wang, S. Han, M. Fang, X. Liu, W. Liu, P. Cao, Nanomaterials. **13**, 1422 (2023). [doi]
24. S. Zhang, L. Weng, B. Liu, D. Kuang, X. Liu, B. Jiang, G. Zhang, Z. Bao, G. Yuan, J. Guo, Vacuum. **215**, 112225 (2023). [doi]
25. Y.-S. Kim, W.-B. Lee, H.-J. Oh, T. Hong, J.-S. Park, Adv. Mater. Interfaces. **9**, 2200501 (2022). [doi]
26. X. Ji, Y. Yuan, X. Yin, S. Yan, Q. Xin, A. Song, IEEE Trans. Electron. Devices. **69**, 6783 (2022). [doi]
27. W. Xu, G. Zhang, X. Feng, J. Alloys Compd. **862**, 158030 (2021). [doi]
28. M.M. Billah, A.B. Siddik, J.B. Kim, D.K. Yim, S.Y. Choi, J. Liu, D. Severin, M. Hanika, M. Bender, J. Jang, Adv. Electron. Mater. **7**, 2000896 (2021). [doi]
29. S.-L. Li, M.-X. Lee, C.-C. Yen, T.-L. Chen, C.-H. Chou, C. Liu, in *2021 International Symposium on VLSI Technology, Systems and Applications (VLSI-TSA)* IEEE, (2021), pp. 1
30. J.-L. Weng. [doi]
31. W. Huo, Z. Mei, Y. Lu, Z. Han, R. Zhu, T. Wang, Y. Sui, H. Liang, X. Du, Chin. Phys. B **28**, 087302 (2019). [doi]
32. S.I. Kim, C.J. Kim, J.C. Park, I. Song, S.W. Kim, H. Yin, E. Lee, J.C. Lee, Y. Park, in 2008 *IEEE International Electron Devices Meeting* (IEEE, 2008), pp. 1
33. C. Peng, M. Xu, L. Chen, X. Li, J. Zhang, Jpn. J. Appl. Phys. **61**, 070914 (2022). [doi]
34. M.M. Billah, M.D.H. Chowdhury, M. Mativenga, J.G. Um, R.K. Mruthyunjaya, G.N. Heiler, T.J. Tredwell, J. Jang, IEEE Electron Device Lett. **37**, 735 (2016). [doi]
35. J.-H. Yang, J.H. Choi, S.H. Cho, J.-E. Pi, H.-O. Kim, C.-S. Hwang, K. Park, S. Yoo, IEEE Electron Device Lett. **39**, 508 (2018). [doi]
36. A. Flewitt, M. Powell, J. Appl. Phys. **115** (2014). [doi]
37. M. Chun, M.D.H. Chowdhury, J. Jang, AIP Adv. **5** (2015). [doi]
38. S. Priyadarshi, M.M. Billah, T. Lim, S.S. Urmi, J. Jang, IEEE Electron Device Lett. **44**, 428 (2023). [doi]
39. J. Kim, J. Park, G. Yoon, A. Khushabu, J.-S. Kim, S. Pae, E.-C. Cho, J. Yi, *Materials Science in Semiconductor Processing* 120, 105264%U https://linkinghub.elsevier.com/retrieve/pii/S1369800120311999 (2020). [doi]
40. W.-S. Liu, C.-L. Huang, Y.-H. Lin, C.-H. Hsu, Y.-M. Chu, Semicond. Sci. Technol. **35**, 025004 (2019). [doi]
41. M.H. Cho, H. Seol, A. Song, S. Choi, Y. Song, P.S. Yun, K.-B. Chung, J.U. Bae, K.-S. Park, J.K. Jeong, IEEE Trans. Electron. Devices. **66**, 1783 (2019). [doi]
42. P.O. Oviroh, R. Akbarzadeh, D. Pan, R.A.M. Coetzee, T.-C. Jen, Sci. Technol. Adv. Mater. **20**, 465 (2019). [doi]
43. J.-Y. Huh, J.-H. Jeon, H.-H. Choe, K.-W. Lee, J.-H. Seo, M.-K. Ryu, S.-H.K. Park, C.-S. Hwang, W.-S. Cheong, Thin Solid Films. **519**, 6868 (2011). [doi]
44. D.G. Yang, H. Do Kim, J.H. Kim, S.W. Lee, J. Park, Y.J. Kim, H.-S. Kim, Thin Solid Films. **638**, 361 (2017). [doi]
45. T. Pi, D. Xiao, H. Yang, G. He, X. Wu, W. Liu, D.W. Zhang, S.-J. Ding, IEEE Trans. Electron. Devices. **69**, 156 (2021). [doi]
46. C. Peng, S. Yang, C. Pan, X. Li, J. Zhang, IEEE Trans. Electron. Devices. **67**, 4262 (2020). [doi]
47. Y. Nam, H.-O. Kim, S.H. Cho, S.-H.K. Park, RSC Adv. **8**, 5622 (2018). [doi]
48. T. Song, D. Zhang, M. Wang, IEEE Electron Device Lett. **42**, 1623 (2021). [doi]
49. Y. Wei, Y. Yu, N. Lv, D. Zhang, M. Wang, R. Wang, L. Lu, M. Wong, IEEE Trans. Electron. Devices. **68**, 1649 (2021). [doi]
50. K.-M. Jung, J. Oh, H.E. Kim, A. Schuck, K. Kim, K. Park, J.-H. Jeon, S.-Y. Lee, Y.-S. Kim, J. Phys. D **53**, 355107 (2020). [doi]
51. Y. Li, J. Sun, T. Salim, R. Liu, T. Chen, ECS J. Solid State Sci. Technol. **10**, 045006 (2021). [doi]
52. K.Y. Shin, Y.J. Tak, W.-G. Kim, S. Hong, H.J. Kim, ACS Appl. Mater. Interfaces. **9**, 13278 (2017). [doi]

53. J. Chen, C.T. Liu, Ieee Access. **1**, 150 (2013). [doi]
54. H.-J. Shin, S.-H. Choi, D.-M. Kim, S.-E. Han, S.-J. Bae, S.-K. Park, H.-S. Kim, C.-H. Oh, in *SID Symposium Digest of Technical Papers* Wiley Online Library, (2021), pp. 611
55. Y. Takeda, S. Kobayashi, S. Murashige, K. Ito, I. Ishida, S. Nakajima, H. Matsukizono, N. Makita, in *SID Symposium Digest of technical papers* Wiley Online Library, (2019), pp. 516
56. M. Ito, M. Kon, M. Ishizaki, N. Sekine, *Proc. IDW/AD* 5, 845 (2005). [doi]
57. S. Nakano, N. Saito, K. Miura, T. Sakano, T. Ueda, K. Sugi, H. Yamaguchi, I. Amemiya, M. Hiramatsu, A. Ishida, J. Soc. Inform. Display. **20**, 493 (2012). [doi]
58. J.-S. Kim, J.-W. Byun, J.-H. Jang, Y.-D. Kim, K.-L. Han, J.-S. Park, B.-D. Choi, IEEE Trans. Electron. Devices. **65**, 3269 (2018). [doi]
59. B. Han, H. Li, G. Li, P. Zhang, X. Yang, S. Qin, R. Huang, Z. Chen, H. Zhang, Y. Hsu, (Wiley Online Library, 2023), pp. 77
60. M.T. Vijjapu, S. Surya, M. Zalte, S. Yuvaraja, M.S. Baghini, K.N. Salama, *Sensors and Actuators B: Chemical* 331, 129450%@ 0925 (2021). [doi]
61. W. Jiang, C. Peng, Y. Yuan, S. Yang, X. Li, J. Mater. Sci.: Mater. Electron. **31**, 1547 (2020). [doi]